2007

Artemisinin induces calcium-dependent protein secretion in the protozoan parasite Toxoplasma gondii

Kisaburo Nagamune
Washington University School of Medicine in St. Louis

Wandy L. Beatty
Washington University School of Medicine in St. Louis

L. David Sibley
Washington University School of Medicine in St. Louis

Eukaryotic
Cell

Updated information and services can be found at:
http://ec.asm.org/content/6/11/2147

These include:

SUPPLEMENTAL MATERIAL   Supplemental material

REFERENCES   This article cites 50 articles, 24 of which can be accessed free
at: http://ec.asm.org/content/6/11/2147#ref-list-1

CONTENT ALERTS   Receive: RSS Feeds, eTOCs, free email alerts (when new
articles cite this article), more»

Information about commercial reprint orders: **http://journals.asm.org/site/misc/reprints.xhtml**
To subscribe to to another ASM Journal go to: **http://journals.asm.org/site/subscriptions/**

Journals.ASM.org

Artemisinin Induces Calcium-Dependent Protein Secretion in the Protozoan Parasite *Toxoplasma gondii*[∇][†]

Kisaburo Nagamune, Wandy L. Beatty, and L. David Sibley*

Department of Molecular Microbiology, Washington University School of Medicine, 660 S. Euclid Ave., St. Louis, Missouri 63110

Intracellular calcium controls several crucial cellular events in apicomplexan parasites, including protein secretion, motility, and invasion into and egress from host cells. The plant compound thapsigargin inhibits the sarcoplasmic-endoplasmic reticulum calcium ATPase (SERCA), resulting in elevated calcium and induction of protein secretion in *Toxoplasma gondii*. Artemisinins are natural products that show potent and selective activity against parasites, making them useful for the treatment of malaria. While the mechanism of action is uncertain, previous studies have suggested that artemisinin may inhibit SERCA, thus disrupting calcium homeostasis. We cloned the single-copy gene encoding SERCA in *T. gondii* (TgSERCA) and demonstrate that the protein localizes to the endoplasmic reticulum in the parasite. In extracellular parasites, TgSERCA partially relocalized to the apical pole, a highly active site for regulated secretion of micronemes. TgSERCA complemented a calcium ATPase-defective yeast mutant, and this activity was inhibited by either thapsigargin or artemisinin. Treatment of *T. gondii* with artemisinin triggered calcium-dependent secretion of microneme proteins, similar to the SERCA inhibitor thapsigargin. Artemisinin treatment also altered intracellular calcium in parasites by increasing the periodicity of calcium oscillations and inducing recurrent, strong calcium spikes, as imaged using Fluo-4 labeling. Collectively, these results demonstrate that artemisinin perturbs calcium homeostasis in *T. gondii*, supporting the idea that Ca^{2+}-ATPases are potential drug targets in parasites.

Apicomplexan parasites infect a wide range of animals, including humans, using a process of active penetration of their host cells (41). This important group of parasites includes *Plasmodium* spp., the causative agents of malaria, and the opportunistic pathogens *Cryptosporidium* spp. and *Toxoplasma gondii*. Host cell invasion by these parasites relies on regulated secretion of adhesins from apical secretory organelles called micronemes (3). Microneme secretion in *T. gondii* is governed by changes in cytosolic calcium ($[Ca^{2+}]_i$) levels in the parasite, which control gliding motility, cell invasion, and egress (6, 27, 34, 48). Similar studies have demonstrated a role for $[Ca^{2+}]_i$ in secretion and motility by *Cryptosporidium parvum* (7) and *Plasmodium berghei* (14). Although these previous studies indicate an important role for alterations in $[Ca^{2+}]_i$), the molecular mechanisms controlling calcium signaling in parasites are not well understood.

In eukaryotic cells, $[Ca^{2+}]_i$ is maintained at an ~10,000 lower level than the extracellular environment (1). A system of calcium channels and pumps maintains this steep gradient and allows for selective increases in $[Ca^{2+}]_i$, which function as a second messenger (1). Apicomplexans are also capable of maintaining a steep calcium gradient with low resting levels of $[Ca^{2+}]_i$. Quantitative measurements using fura-2 in *T. gondii* indicate that $[Ca^{2+}]_i$ levels are ~100 nM in resting cells (33). Apicomplexans possess several stores of calcium, including acidocalcisomes, the mitochondrion, and the endoplasmic reticulum (ER) (32). Of these potential calcium stores, the ER is the most likely source for rapid release and reuptake of calcium needed to control secretion and motility. Previous studies using pharmacological inhibitors indicate that *T. gondii* responds to agonists of both IP_3 and ryanodine-type receptors and that stimulation of these channels releases Ca^{2+} and stimulates parasite gliding and microneme secretion (8, 26). Perturbation of $[Ca^{2+}]_i$ levels not only blocks secretion but also prevents motility and cell invasion (27). Fluorescent imaging studies using calcium-sensitive dyes have revealed that $[Ca^{2+}]_i$ levels in the parasite oscillate during parasite gliding (27, 49) and are elevated during host cell contact (48). However, a prolonged increase of calcium is toxic as shown by treatment with caffeine, which elevates $[Ca^{2+}]_i$ and abolishes the natural oscillations in calcium seen in motile parasites (49). These findings indicate an important role for reuptake of calcium to dampen signaling and refill intracellular stores.

Recent phylogenetic analysis of the apicomplexan genomes (i.e., *Plasmodium*, *Cryptosporidium*, and *Toxoplasma*) indicates highly conserved complement of P-type Ca^{2+} ATPases (36). These particular apicomplexans contain a single orthologue each of the sarcoplasmic ER Ca^{2+} ATPase (SERCA), also referred to as ATPase6 in *P. falciparum* (21). These apicomplexans also contain an orthologue of the yeast PMR1 transporter (36), which has previously been called ATPase4 in *P. falciparum*, where it is reported to localize to the plasma membrane of asexual stages (11). In addition, apicomplexans contain several additional Golgi-ER-type Ca^{2+} ATPases and a single Ca^{2+}/H^+ exchanger (36). The precise roles played by these Ca^{2+} ATPases in calcium homeostasis and signaling have not been addressed by functional studies. Uniquely, *T. gondii*

* Corresponding author. Mailing address: Department of Molecular Microbiology, Washington University School of Medicine, 660 S. Euclid Ave., St. Louis, MO 63110. Phone: (314) 362-8873. Fax: (314) 286-0060. E-mail: sibley@borcim.wustl.edu.

contains two plasma membrane-type Ca^{2+} ATPases, which are apparently absent from *Plasmodium* and *Cryptosporidium*. One of these genes, *TgA1* (named for *T. gondii* plasma membrane calcium ATPase 1), has previously been characterized as a component of both the plasma membrane and the acidocalcisome (29). Disruption of *TgA1* leads to decreased polyphosphate content, increases in basal $[Ca^{2+}]_i$, and impaired invasion (28), demonstrating that calcium homeostasis is critical for intracellular survival.

SERCA is one of best characterized P-type ATPases, which are defined by the existence of a phosphorylated intermediate during their catalytic cycle (50). Each SERCA protein transports two Ca^{2+} ions from the cytoplasm to the lumen of the ER using the energy from hydrolysis of one ATP molecule (44). SERCA consists of 10 transmembrane regions (M1 to M10) and three cytoplasmic domains (A domain, actuator; N domain, nucleotide binding; and P domain, phosphorylation) (46). The reaction mechanism involves transformation between two conformational states known as E1 and E2, resulting in binding of calcium on the cytoplasmic side and release into the lumen of the ER (44, 50). Thapsigargin, a sesquiterpene lactone produced by the plant *Thapsia garganica*, locks the protein in the E2 form, which has a lower affinity for calcium, thus blocking activity (38, 39, 43).

Artemisinin is also a sesquiterpene lactone that is produced by the plant *Artemisia annua*. Artemisinin and related compounds such as artemether and artesunate contain an endoperoxide ring that is crucial for activity (18). In *Plasmodium*, the SERCA orthologue, PfATP6, was proposed as a target of the antimalarial drug artemisinin, based on heterologous expression studies in *Xenopus* oocytes (12). Artemisinins also disrupt the growth of *Trypanosoma cruzi* and inhibit calcium-dependent ATPase activity in membrane fractions from the parasite (31). Artemisinin and related compounds are also effective against *T. gondii* in vitro; however, they are not used clinically to treat toxoplasmosis due to relatively low efficacy (19, 20, 40).

To explore the molecular mechanism of inhibition by artemisinin, we cloned the SERCA homologue of *T. gondii* (TgSERCA), demonstrated it functions as a Ca^{2+} ATPase, and tested its sensitivity to artemisinin.

MATERIALS AND METHODS

Compounds. Artemisinin (98% pure) (CID: 452191), thapsigargin (>90% pure) (CID: 5321923), and caffeine (98% pure) (CID: 64119) were obtained from Sigma (St. Louis, MO). BAPTA and BAPTA-AM (>95% pure) were obtained from Molecular Probes (Invitrogen, Carlsbad, CA). Compounds were dissolved in dimethyl sulfoxide (DMSO; Sigma) and stored at −80C until use.

Parasites and culture. *T. gondii* strain RH (ATCC 50838), clone 2F (ATCC 50839) that expresses bacterial β-galactosidase (10) was propagated as tachyzoites in human foreskin fibroblast cells (HFF) grown in D10 medium (Dulbecco modified Eagle medium, 10 mM HEPES, 44 mM sodium bicarbonate, 10% fetal bovine serum, 2 mM glutamine, 10 μg/ml of gentamicin).

Assay for mitochondrial membrane potential. Purified parasites were treated with artemisinin in normal growth medium for 2 to 6 h and washed three times with phosphate-buffered saline (PBS) containing 100 μM $CaCl_2$ by centrifugation at $400 \times g$ for 10 min. Parasite cells were resuspended in 1 ml of PBS containing 2 mM $CaCl_2$ with 2 μM rhodamine-123 (Invitrogen/Molecular Probes), incubated for 30 min at room temperature, washed three times, and resuspended in PBS containing calcium. Mitochondrial electrochemical potential was monitored by using a FACSCalibur instrument (Becton Dickinson Biosciences, San Jose, CA) (excitation at 480 nm and emission at 530 nm).

Cloning of TgSERCA. TgSERCA was identified by BLASTX search against the *T. gondii* genome database (http://www.toxodb.org/) using SERCA homologues from human (GenBank no. NP_775293), *Arabidopsis thaliana* (NP_191999), and *Plasmodium falciparum* (Q08853) as query sequences. The full-length cDNA was cloned from the RH strain (ATCC 50838) using the SMART RACE cDNA amplification kit (Clontech, Mountain View, CA). Predicted amino acid sequences were aligned by CLUSTAL W (http://www.ebi.ac.uk/clustalw/). Hydrophobicity profiles were analyzed by using the Kyte and Doolittle method (http://bioinformatics.weizmann.ac.il/hydroph/plot_hydroph.html). Transmembrane regions were predicted by the TMPRED program (http://www.ch.embnet.org/software/TMPRED_form.html), and the domain structures were analyzed by InterProScan (http://www.ebi.ac.uk/InterProScan/).

Yeast complementation. *Saccharomyces cerevisiae* strain K616 (9) was transformed with *TgSERCA*/pYES2 or empty vector and grown in liquid uracil-deficient synthetic complete medium at 30°C overnight. The allele of TgSERCA that was used for yeast expression studies differed in several residues (N562S, L1043P) from the GenBank entry for TgSERCA (AAU93917). These differences were presumably due to mutations acquired during PCR amplification of cDNA; however, since they do not occur in critical residues they were not repaired. Cells were inoculated into medium with galactose as a carbon source instead of glucose at an initial optical density at 600 nm (OD_{600}) of 0.01. EGTA, or EGTA plus thapsigargin, artemisinin, or caffeine were added to the medium and cultures were incubated 24 to 48 h at 30°C. After the incubation, growth was measured by absorbance at OD_{600}. Each experiment was repeated three times, and differences in the means were compared by using the Student *t* test.

Fluo-4 calcium monitoring. Calcium monitoring was conducted using Fluo-4 as described previously (27, 49). Briefly, freshly egressed parasites were labeled with 250 nM Fluo-4-AM (Molecular Probes) for 5 to 10 min at room temperature, followed by centrifugation at $400 \times g$ for 5 min and washing in Ringer's solution. Parasites were resuspended in Ringer's solution containing 2 mM $CalCl_2$ and 1% fetal bovine serum (FBS) and treated with 10 to 50 μM artemisinin, 0.5 to 1.0 μM thapsigargin, or 1% DMSO as a control. After the addition of drug, cells were added directly to 35-mm glass-bottom microwell dishes (MatTek, Ashland, MA) and imaged over a 15- to 20-min period using a temperature-controlled stage (Medical Systems, Greenvale, NY). Cells were examined by using epifluorescence illumination with a 100-W mercury source on a Axiovert microscope equipped with a fluorescein isothiocyanate filter set (XF23; Omega Optical, Brattleboro, VT) using a 63× lens (NA 1.35). Images were captured at five frames/second by using an Orca ER low-light level camera (Hamamatsu, Inc., Japan) using Openlab v 4.1 (Improvision, Lexington, MA) software. Quantitative analysis of image pixel intensity was performed by using Openlab measurement module and graphed in Excel.

Expression of recombinant protein and generation of anti-TgSERCA antibody. The P and N domains of *TgSERCA* (nucleotides 1117 to 2415, corresponding to amino acid residues 373 to 805) were cloned into the NdeI-HindIII sites of pET-22b(+) (EMD Biosciences Novagen, La Jolla, CA) to generate fusions containing a C-terminal His$_6$ tag. Expression was induced in *Escherichia coli* BL21 by the addition of 1 mM IPTG (isopropyl-β-D-thiogalactopyranoside) for 24 h at 25°C, and the resulting protein was purified by using the ProBond purification system (Invitrogen). CD1 outbred mice were immunized with 10 μg each of purified polypeptide and Freund complete adjuvant (Sigma-Aldrich, St. Louis, MO), followed by two boosts of antigen in incomplete adjuvant. SERCA was detected in parasite or HFF lysates that were resolved on SDS-PAGE and Western blotted with antibodies to TgSERCA (dilution 1:15,000). Signals were detected using goat anti-mouse or goat anti-rabbit conjugated to horseradish peroxidase (dilution 1:10,000; Jackson Immunoresearch Laboratories, West Grove, PA) and SuperSignal West Pico (Pierce, Rockford, IL).

Immunofluorescence microscopy. Intracellular and extracellular parasites were processed for immunofluorescence microscopy as described previously (27). Briefly, cells were fixed with 4% formaldehyde for 20 min, permeabilized by 0.5% Triton X-100, and blocked in 10% FBS in PBS. Mouse anti-TgSERCA antiserum was used at 1:5,000 dilution. Anti-yeast V-ATPase 100-kDa subunit monoclonal antibody 10D7 (Invitrogen/Molecular Probes) was used at a 1:100 dilution. RH strain expressing green fluorescent protein (GFP)-HDEL was provided by Kristen Hager (Notre Dame University). *T. gondii* was incubated with a MitoTracker (Molecular Probes; final concentration, 0.5 μM) in D10 at 37°C for 45 min and then rinsed three times with 5 ml of fresh D10 at 37°C for 5 min. Samples were examined on a Axioscop-2 Mot Plus microscope (Carl Zeiss, Thornwood, NJ) equipped for epifluorescence microscopy (DAPI [4′,6′-diamidino-2-phenylindole], fluorescein isothiocyanate, and Texas Red filter cubes [Chroma Technology Corp., Rockingham, VT]). Images were acquired by using a 1.4 NA 100× Plan-Apochromat lens, captured by an AxioCam MRm CCD

(Zeiss), and processed by using Axiovision software v4.5 (Zeiss). Images were deconvolved by using an inverse filter algorithm.

Electron microscopy. For immuno-electron microscopy, parasites were fixed in 4% paraformaldehyde (Polysciences, Inc., Warrington, PA) in 100 mM phosphate buffer (pH 7.2) for 30 min at room temperature. Immunolabeling and silver enhancement were carried out prior to embedding as follows. Fixed parasites were washed in blocking buffer (5% FBS, 5% normal goat serum, 0.05% saponin, 100 mM phosphate) and subsequently incubated for 30 min with mouse anti-SERCA or rabbit anti-GFP antibodies (ab6556; AbCam, Inc., Cambridge, MA) diluted in blocking buffer. Samples were washed in phosphate buffer and probed for 30 min with nanogold anti-mouse or anti-rabbit conjugates (Nanoprobes, Yaphank, NY) diluted in blocking buffer. Samples were washed in phosphate buffer and fixed for 15 min with 1% glutaraldehyde (Polysciences) in phosphate buffer. Samples were silver enhanced for 10 min by using an LI silver enhancement kit (Nanoprobes), washed in water, embedded in 10% gelatin, and infiltrated overnight with 2.3 M sucrose and 20% polyvinylpyrrolidone in PIPES [piperazine-*N,N*′-bis(2-ethanesulfonic acid)]–MgCl₂ at 4°C. Samples were trimmed, frozen in liquid nitrogen, and sectioned with a Leica Ultracut UCT cryo-ultramicrotome (Leica Microsystems, Inc., Bannockburn, IL). Ultrathin sections (~70 nm) were stained with 0.3% uranyl acetate and 2% methylcellulose and then viewed with a JEOL 1200EX transmission electron microscope (JEOL USA, Inc., Peabody, MA).

MIC2 secretion assay. Microneme secretion assays were performed as described previously (5, 26). Briefly, freshly egressed parasites were suspended in assay medium (Dulbecco modified Eagle medium with 44 mM sodium bicarbonate, 20 mM HEPES, 2 mM glutamine, 10 μg of gentamicin/ml, and 3% FBS) and treated with different concentrations of calcium agonists for 5 or 10 min at 18°C. In some experiments, parasites were pretreated with 50 μM BAPTA-AM or 1 mM BAPTA (Molecular Probes) for 20 min at 18°C to chelate intracellular and extracellular calcium, respectively, or with DMSO. Treated cells were then incubated for 10 min at 18°C with 10 μM artemisinin or 1% ethanol as a positive control. After treatments, parasites were transferred to 37°C for 2 min to allow secretion, chilled on wet ice, and separated into the supernatant and cell pellet by centrifugation at 400 × *g*. Proteins were resolved by sodium dodecyl sulfate-15% polyacrylamide gel electrophoresis, transferred onto nitrocellulose membranes, and Western blotted with rabbit anti-MIC2 antibody (1:10,000) or mouse anti-β-galactosidase monoclonal antibody 40a-1 (1:300) and horseradish peroxidase-conjugated goat anti-rabbit or mouse immunoglobulin G (IgG) (1:10,000) (Jackson Immunoresearch Laboratories, West Grove, PA). Signals were detected by using SuperSignal West Pico (Pierce).

RESULTS

Characterization of TgSERCA. To identify the SERCA orthologue from *T. gondii* (*TgSERCA*), *A. thaliana*, and *P. falciparum* SERCA orthologues were used to search the *T. gondii* genome database (http://www.toxodb.org/) using TBLASTN. A single SERCA homologue identified in *T. gondii* (Draft 3 annotation 44.m02594) shared more than 50% identity with human, plant, and *Plasmodium* orthologues (see Fig. S1 in the supplemental material). The full-length sequence was determined from amplified cDNA of the RH strain and the resulting predicted protein sequence was deposited in GenBank (AAU93917). Comparison of the predicted secondary structures and domain architectures revealed that TgSERCA contained 10 transmembrane regions similar to human and *Plasmodium* orthologues (Fig. 1A). TgSERCA also contained conserved domains found in E1-E2 type calcium ATPases, including a cation-transporting ATPase N-terminal domain (InterProScan: IPR004014), an E1-E2 ATPase domain (IPR008250), a haloacid dehalogenase-like hydrolase domain (IPR005834), and a cation-transporting ATPase C-terminal domain (IPR006068, Fig. 1B). TgSERCA also contained conserved amino acid residues that are predicted to form the Ca²⁺-binding and ATP-binding pockets (42, 45, 46) (Fig. 1B).

Localization of TgSERCA to the ER in *T. gondii*. To investigate the localization of TgSERCA, we generated an anti-
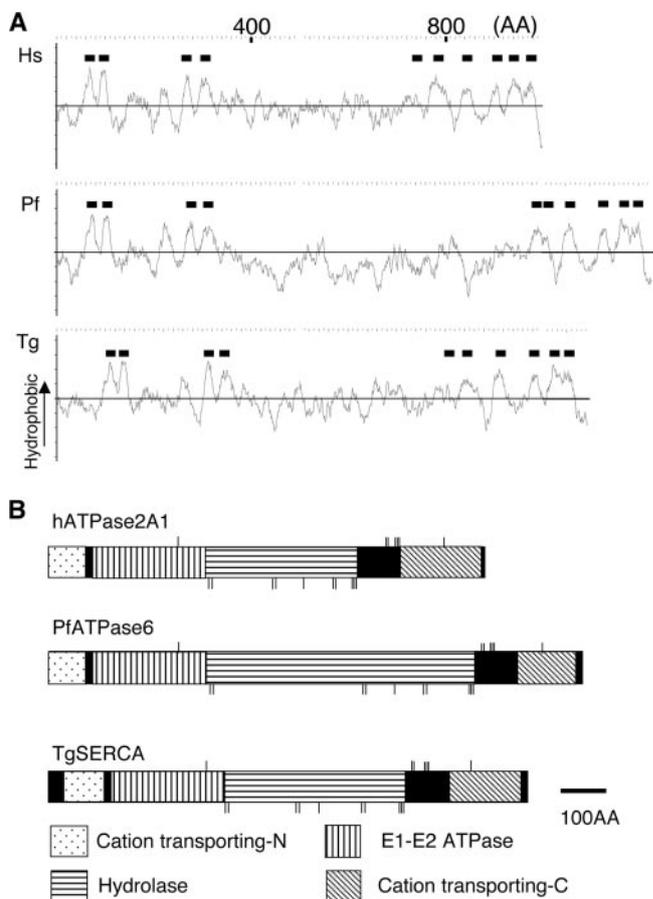

FIG. 1. Predicted secondary structure and conserved domains found in TgSERCA. (A) Hydrophobicity profiles of human ATPase2A1 (Hs), *P. falciparum* ATPase6 (Pf), and TgSERCA (Tg). Black bars indicate putative transmembrane regions. (B) Predicted domain structure of human ATPase2A1 (hATPase2A1), *P. falciparum* ATPase6 (PfATPase6), and TgSERCA. Cation-transporting ATPase N-terminal domain (Cation transporting-N), E1-E2 ATPase domain, haloacid dehalogenase-like hydrolase domain (Hydrolase), and cation-transporting ATPase C-terminal domain (Cation transporting-C) are shown. Thin vertical bars indicate the essential amino acid residues that form the Ca²⁺-binding pocket (upper bars) and residues that interact with ATP (lower bars). Scale bar, 100 amino acids (100AA).

TgSERCA polyclonal antiserum to the phosphorylation (P) and nucleotide binding (N) domains expressed as a recombinant protein in *E. coli* (see Materials and Methods). Anti-TgSERCA sera recognized a single band in parasite cells at around 120 kDa, which corresponds to the estimated M_r of TgSERCA, but did not cross-react with host cells by Western blotting (Fig. 2A). Anti-TgSERCA antiserum was used for immunofluorescence microscopy of the *T. gondii* RH strain expressing GFP-HDEL, which serves as an ER marker (17). In intracellular parasites, TgSERCA and GFP-HDEL were localized primarily surrounding the nucleus of the parasite and extending into the cytoplasm (Fig. 2B). The characteristic pattern of this staining and colocalization with GFP-HDEL indicated that TgSERCA is likely localized in the ER in intracellular parasites. However, in extracellular parasites, TgSERCA had partially relocalized to the apical region in a pattern that was nonoverlapping with GFP-HDEL (Fig. 2C). A similar re-
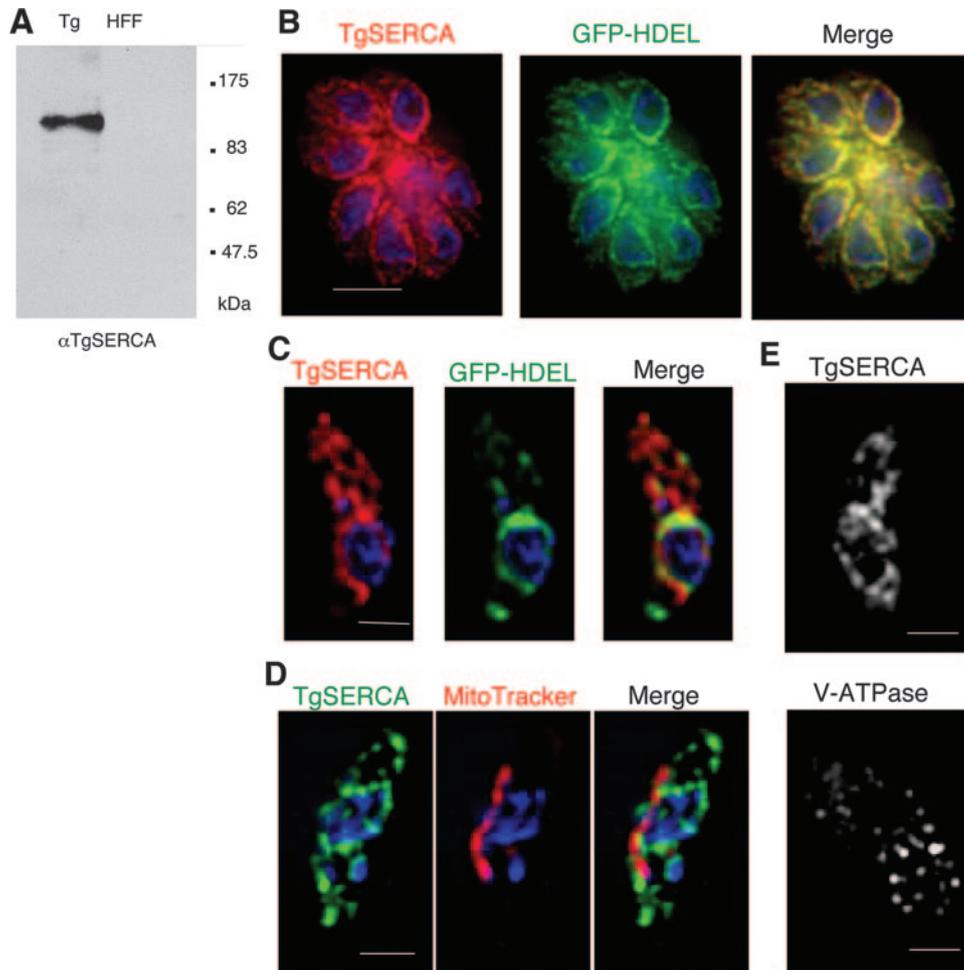
FIG. 2. Localization of TgSERCA in *T. gondii*. (A) Western blot with anti-TgSERCA antibody against *T. gondii* lysate (Tg) revealed a single band of 120 kDa, while HFF cell lysate (HFF) was negative. (B) Immunofluorescence staining of intracellular *T. gondii*. Intracellular parasites expressing GFP-HDEL were stained with anti-TgSERCA, followed by Alexa-594-conjugated goat anti-mouse IgG (red). The middle panel shows the signal of GFP-HDEL (green), with a merged image shown at the right. Nuclei were stained with DAPI (blue). Bar, 5 μm. (C) Localization of TgSERCA and GFP-HDEL in extracellular parasites. Panels: left, anti-TgSERCA (red, stained as in panel B); middle, GFP-HDEL (green); right, merged image. Nuclei were stained with DAPI (blue). Bar, 2 μm. (D) Localization of TgSERCA and mitochondrion in extracellular parasites. Panels: left, stained with mouse anti-TgSERCA followed by Alexa-488-conjugated goat anti-mouse IgG (green); middle, MitoTracker (red), right, merged image. Nuclei were stained with DAPI (blue). Bar, 2 μm. (E) Localization of TgSERCA (upper) and acidocalcisomes (lower) in separate extracellular parasites. The upper panel was stained with mouse anti-TgSERCA, followed by goat anti-mouse IgG; the lower panel was stained with anti-V-ATPase, followed by goat anti-mouse IgG. Bar, 2 μm. Wide field images were acquired and deconvolved as described in Materials and Methods. A single mid-Z plane is shown for each example.

sult was obtained using anti-GFP antibody to localize GFP-HDEL (data not shown).

The distribution pattern of SERCA in *T. gondii* parasites does not resemble micronemes, rhoptries or dense granules, a result confirmed by electron microscopy below. To determine whether the vesicular structures stained with anti-TgSERCA were mitochondria, we costained *T. gondii* parasites with anti-TgSERCA antibody and the mitochondrial marker, Mito-Tracker. The mitochondrion in *T. gondii* was observed as single tube-like structure as reported previously (30), and this signal did not colocalize with that of anti-TgSERCA antibody (Fig. 2D). Furthermore, we investigated whether the staining pattern of TgSERCA was similar to acidocalcisomes, which contain high levels of Ca^{2+} (29). The staining pattern with anti-vacuolar-ATPase, an acidocalcisome marker (29), revealed

small punctate vesicles that did not appear to be similar to the extended membranous structures stained with anti-TgSERCA (Fig. 2E). Although we were unable to perform costaining studies due to the fact that both antibodies were produced in mice, we interpret this result to indicate that TgSERCA is not localized appreciably to acidocalcisomes. Collectively, these results indicate that in intracellular parasites TgSERCA was largely localized in the ER with GFP-HDEL, whereas in extracellular parasites TgSERCA was partially relocalized in a distinct apical membrane compartment.

To further explore the localization of TgSERCA, we performed cryo-immuno-electron microscopy labeling of *T. gondii*. The epitopes recognized by the mouse anti-TgSERCA proved to be extremely sensitive to fixation, precluding post-processing immunolabeling (data not shown). Instead, we

lightly fixed cells, permeabilized them, and performed immunolabeling and silver enhancement prior to embedding (see Materials and Methods). Staining of TgSERCA confirmed that in intracellular parasites it was localized in the nuclear envelope and in ER membranes that surround the nucleus (Fig. 3A). Although the intensity of labeling was slightly lower, GFP-HDEL was also detected in the ER and surrounding the nuclear envelope (Fig. 3C). In extracellular parasites, TgSERCA was partially relocalized to apical membranes in the vicinity of micronemes (arrow, Fig. 3B), while GFP-HDEL remained associated with the nuclear envelope and proximal ER (Fig. 3D). The ultrastructural morphology of secretory organelles in *T. gondii* is quite distinct, and no specific staining of micronemes, dense granules, or rhoptries was observed by cryo-immuno-electron microscopy labeling (Fig. 3D and data not shown). Control sections stained with an isotype control antibody remained negative, confirming the specificity of this technique (Fig. 3E).

Heterologous expression and activity of TgSERCA. To determine whether TgSERCA functions as a Ca^{2+} transporter, we used the yeast mutant strain K616, which is defective in both Golgi (PMR1) and vacuolar (PMC1) Ca^{2+} pumps and also lacks calcineurin (CNB1) (9). Previous reports have shown that plant (25) and trypanosomal (13) SERCA orthologues complement the growth of this mutant yeast strain in low-Ca^{2+} medium. The K616 mutant yeast was transfected with TgSERCA, and growth was observed in low-calcium medium containing EGTA. TgSERCA complemented the growth of the K616 yeast strain in low-Ca^{2+} medium with a maximum effect seen when growth was inhibited by 10 mM EGTA (Fig. 4A). Thapsigargin, which is a potent SERCA inhibitor (38), reversed the growth complementing effect of TgSERCA, while treatment of yeast cells containing a vector control had no effect (Fig. 4B). The complementing effects of TgSERCA were not reversed by treatment with caffeine (Fig. 4C), which does not act directly on TgSERCA, but rather activates a ryanodine-type calcium release channel (26). Caffeine is known to enter yeast cells efficiently and to affect kinase signaling (23), although yeast cells lack ryanodine-responsive calcium channels. We also tested the effects of artemisinin treatment on the ability of TgSERCA to rescue the K616 mutant yeast grown in low calcium. The complementation of K616 yeast mutants grown in low calcium was blocked by treatment with artemisinin (Fig. 4D), a finding consistent with TgSERCA being inhibited by this compound. Yeast cells containing the vector alone were not inhibited by treatment with similar levels of artemisinin (Fig. 4D). These findings support a functional role for TgSERCA in restoring calcium homeostasis in this defective yeast strain. Similar results have been obtained by previous studies that have used this yeast mutant to study Ca^{2+} ATPases from *T. cruzi* (13) and from plants (25).

Artemisinin does not affect mitochondrial membrane potential in *T. gondii*. A recent report indicated that treatment of artemisinin causes substantial loss of mitochondrial membrane potential in *S. cerevisiae*, albeit it at very high concentrations (24). Consequently, we investigated whether a similar event occurs in *T. gondii* using rhodamine-123, which monitors mitochondrial membrane potential. Treatment of *T. gondii* with a high dose of artemisinin (100 μM) for 2 h did not alter membrane potential (Fig. 4E), although significant loss was previ-

ously reported by treatment with 8 μM artemisinin in yeast (24). Furthermore, no difference was observed in the membrane potential of *T. gondii* after incubation with 100 μM artemisinin for 6 h (data not shown). These results indicate that the mitochondrion is not a primary target of artemisinin in *T. gondii*.

Artemisinin induces calcium-dependent secretion in *T. gondii*. Microneme secretion in *T. gondii* is triggered by elevated cytosolic calcium as shown by detection of the soluble form of MIC2 that is shed into the supernatant following release onto the cell surface and proteolytic cleavage (4, 5). Inhibition of TgSERCA by treatment with thapsigargin results in elevated $[Ca^{2+}]_i$, which stimulates microneme secretion (6, 33). We investigated whether treatment with artemisinin would induce a similar exocytic response by examining cell supernatants for the presence of shed MIC2 by Western blotting. Artemisinin induced the secretion of MIC2 in 5 min when treated with 100 μM, while treatment with lower doses (10 μM) required 10 min to detect secretion (Fig. 5A). This effect was similar, albeit less potent, than that seen with thapsigargin or ethanol (4), two positive controls that have been validated in this assay previously (Fig. 5A). The detection of cellular MIC2 in the cell pellet served both as a loading control and to verify that the effects were not due to lysis, which would have resulted in loss from this fraction (Fig. 5A). Next, we tested whether this induction was dependent on cytosolic Ca^{2+}. Secretion of MIC2 by artemisinin was completely reversed by pretreatment with BAPTA-AM, which is a membrane-permeable Ca^{2+} chelator (Fig. 5B). On the other hand, the membrane-impermeable Ca^{2+} chelator, BAPTA, had only a modest affect on secretion (Fig. 5B). These results indicate that artemisinin induces the secretion of microneme proteins through a pathway that is largely dependent on mobilization of intracellular calcium.

Artemisinin induced calcium spikes in *T. gondii*. Previous studies have demonstrated that cytoplasmic calcium levels in *T. gondii* undergo oscillations that are associated with gliding motility (27, 49). We used Fluo-4 imaging to evaluate the effects of artemisinin treatment on intracellular calcium oscillations in *T. gondii*. Fluo-4 has the advantage of being very sensitive and rapid, thus making it ideal for temporal measurements, although it is not ratiometric and thus not useful for measuring calcium concentrations (15). Time-lapse video microscopy was used to monitor temporal changes in intracellular calcium after the addition of artemisinin to Fluo-4-labeled parasites. Representative traces derived from time-lapse recordings are shown in Fig. 6. Treatment with 10 μM artemisinin resulted in rapid, repeated oscillations that showed amplitudes similar to those for control parasites (Fig. 6A) but with an increased periodicity (shorter time between repeated cycles) (Fig. 6B). In parasites treated with 50 μM artemisinin, a second pattern was observed, consisting of strong increases (>4-fold) that appeared quite suddenly and which lasted longer and were spaced further apart (increased period) compared to control cells (Fig. 6B). In previous studies, it was observed that calcium oscillations were most commonly observed in cells undergoing gliding (27). However, artemisinin treatment also induced oscillations in nonmotile cells. A high frequency of total cells responded (up to 50% of the population), and yet responses were not synchronous and at any given time only 5 to 10% of cells exhibited oscillations. Removal of
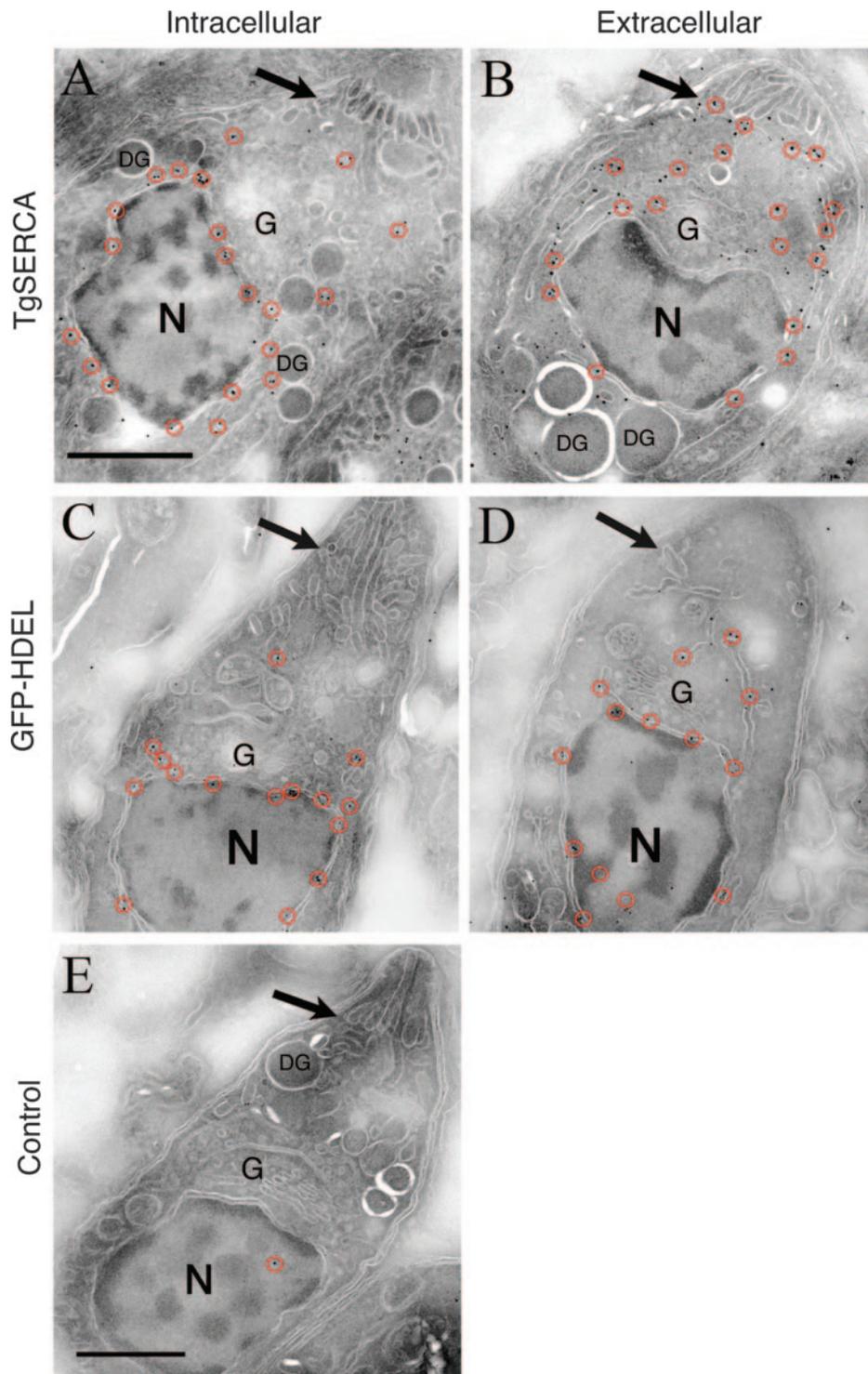
FIG. 3. Immuno-electron microscopy localization of TgSERCA versus GFP-HDEL in *T. gondii*. TgSERCA localized to perinuclear ER in both intracellular and extracellular parasites. In extracellular parasites, SERCA labeling extended into the apical region of parasites where it was associated with vesicular structures (apical region indicated by arrows). (A) Intracellular *T. gondii* immunolabeled with mouse anti-TgSERCA antibody. (B) Extracellular *T. gondii* immunolabeled with mouse anti-TgSERCA antibody. (C) Intracellular *T. gondii* expressing GFP-HDEL immunolabeled with rabbit anti-GFP antibody. (D) Extracellular *T. gondii* expressing GFP-HDEL immunolabeled with rabbit anti-GFP antibody. (E) Intracellular *T. gondii* immunolabeled with isotype control antibody. N, parasite nucleus; DG, dense granules; G, position of the Golgi. Scale bars, 0.5 μm. Note that the variable size of gold particles seen here is due to the silver enhancement technique. To facilitate identification of gold particles, representative clusters are highlighted by red circles.
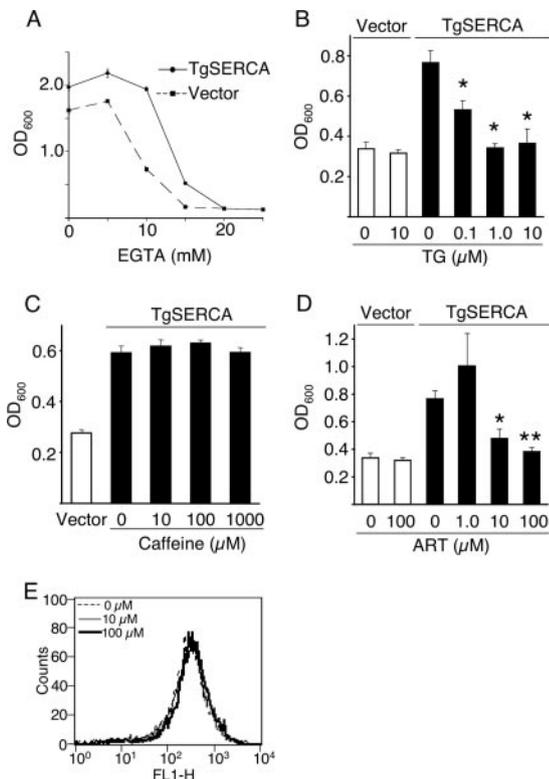
FIG. 4. Complementation of calcium-ATPase deficient yeast strain K616 by *TgSERCA*. (A) Growth of K616 yeast in medium supplemented with EGTA. K616 cells were transformed with *TgSERCA* (solid line) or empty vector (dashed line). Growth was measured by absorbance at OD_{600} after growth for 48 h (see Materials and Methods) with different levels of EGTA. (B) Inhibition of yeast K616 complementation with *TgSERCA* by treatment with thapsigargin. ■, *TgSERCA*; □, empty vector. Transformants were inoculated in medium supplemented with 10 μM EGTA and 0 to 10 μM thapsigargin (TG). Growth was measured at OD_{600} after 24 h of incubation. Asterisk indicates significantly different ($P < 0.02$) versus no thapsigargin. (C) Caffeine did not reverse the complementation of yeast K616 with *TgSERCA*. *TgSERCA* or empty vector transformants were inoculated in medium with 10 μM EGTA and 0 to 1,000 μM caffeine. (D) Inhibition of TgSERCA by artemisinin treatment of yeast K616 mutant. ■, *TgSERCA*; □, empty vector. Transformants of K616 were inoculated in medium supplemented with 10 μM EGTA and 0 to 100 μM artemisinin (ART). Growth was measured at OD_{600} after 24 h of incubation. Single and double asterisks indicate a significant difference ($P \leq 0.05$ and $P \leq 0.01$, respectively) versus no artemisinin. (E) Artemisinin did not affect mitochondrial membrane potential of *T. gondii*. Extracellular parasites were treated with 0 to 100 μM artemisinin (ART) for 2 h and stained with rhodamine-123. The fluorescence intensity was monitored by fluorescence-activated cell sorting, and the FL1-H channel was set to detect rhodamine-123.
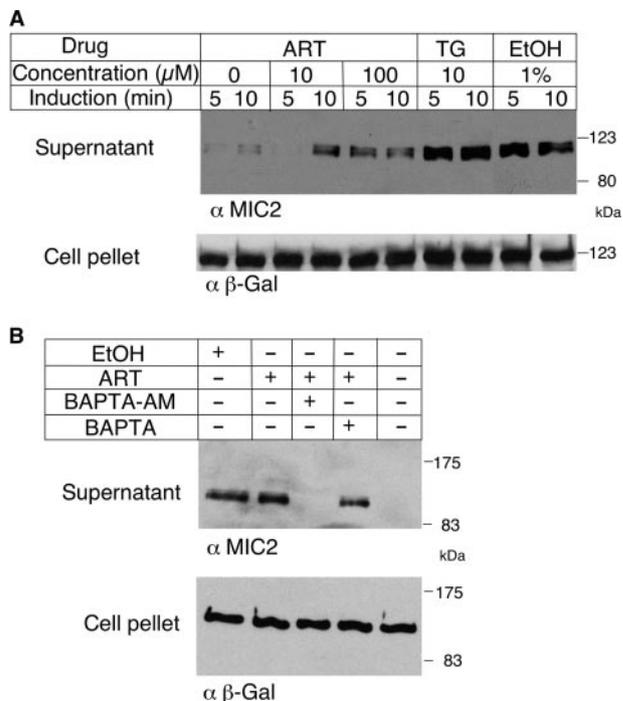

FIG. 5. Induction of MIC2 secretion by extracellular parasites as detected by Western blotting of cell fractions. (A) Treatment with artemisinin causes a dose-dependent release of MIC2 into the supernatant (compare 10 μM versus 100 μM at 5 min). Parasites were pretreated with artemisinin (ART), thapsigargin (TG), or 1% of ethanol (EtOH) for 5 or 10 min at 18°C (to block premature secretion), followed by stimulation of secretion at 37°C for 2 min. Samples were divided into supernatant and cell pellet and analyzed by Western blotting with anti-MIC2 antibody (supernatant) or anti-β-galactosidase (cell pellet). (B) Chelation of intracellular calcium by BAPTA-AM inhibited secretion induced by artemisinin (ART), while chelation of extracellular calcium by BAPTA had minimal effect. Parasites were pretreated with BAPTA or BAPTA-AM at 18°C for 20 min to chelate calcium, followed by treatment with 10 μM artemisinin or 1% ethanol for 10 min at 18°C, and finally stimulation of secretion at 37°C for 2 min, as detailed in Materials and Methods. Samples were analyzed as in panel A.

extracellular calcium from the medium and addition of 5 mM EGTA did not affect the amplitude or periodicity of calcium oscillations in control or artemisinin-treated cells (data not shown), indicating that the source of calcium is from the release of intracellular stores.

In parasites treated with thapsigargin, altered calcium oscillations were also observed (Fig. 6C), although there were several differences from the responses seen with artemisinin. First, the average level of intracellular calcium was elevated by thapsigargin (Fig. 6), a result not seen with artemisinin. Second,

thapsigargin induced both slow calcium spikes with higher amplitude and longer periodicity and short, rapid oscillations (Fig. 6C). Finally, the effects of thapsigargin were noted at doses of 0.5 μM, ≤10-fold lower than similar responses seen with artemisinin (Fig. 6).

To provide a more complete summary of the changes in calcium oscillations, ~25 individual time lapse recordings were analyzed for each condition to determine the time interval between each cycle (period), and the data were plotted as a histogram (Fig. 6D). Changes in the periodicity of calcium oscillations that were induced by artemisinin were very apparent. Treatment with 10 μM artemisinin resulted in a faster periodicity with an average time of 13.95 s (± 4.4) compared to 22.6 s (± 3.5) for control cells (Fig. 6D). In contrast, treatment with 50 μM artemisinin resulted in two responses: cells that responded with average cycle time of 21 to 30 s, similar to controls, and cells that exhibited strong calcium spikes that lasted much longer (Fig. 6D). This biphasic pattern resulted in an average period of 33.8 s (± 15.6). Finally, treatment with low
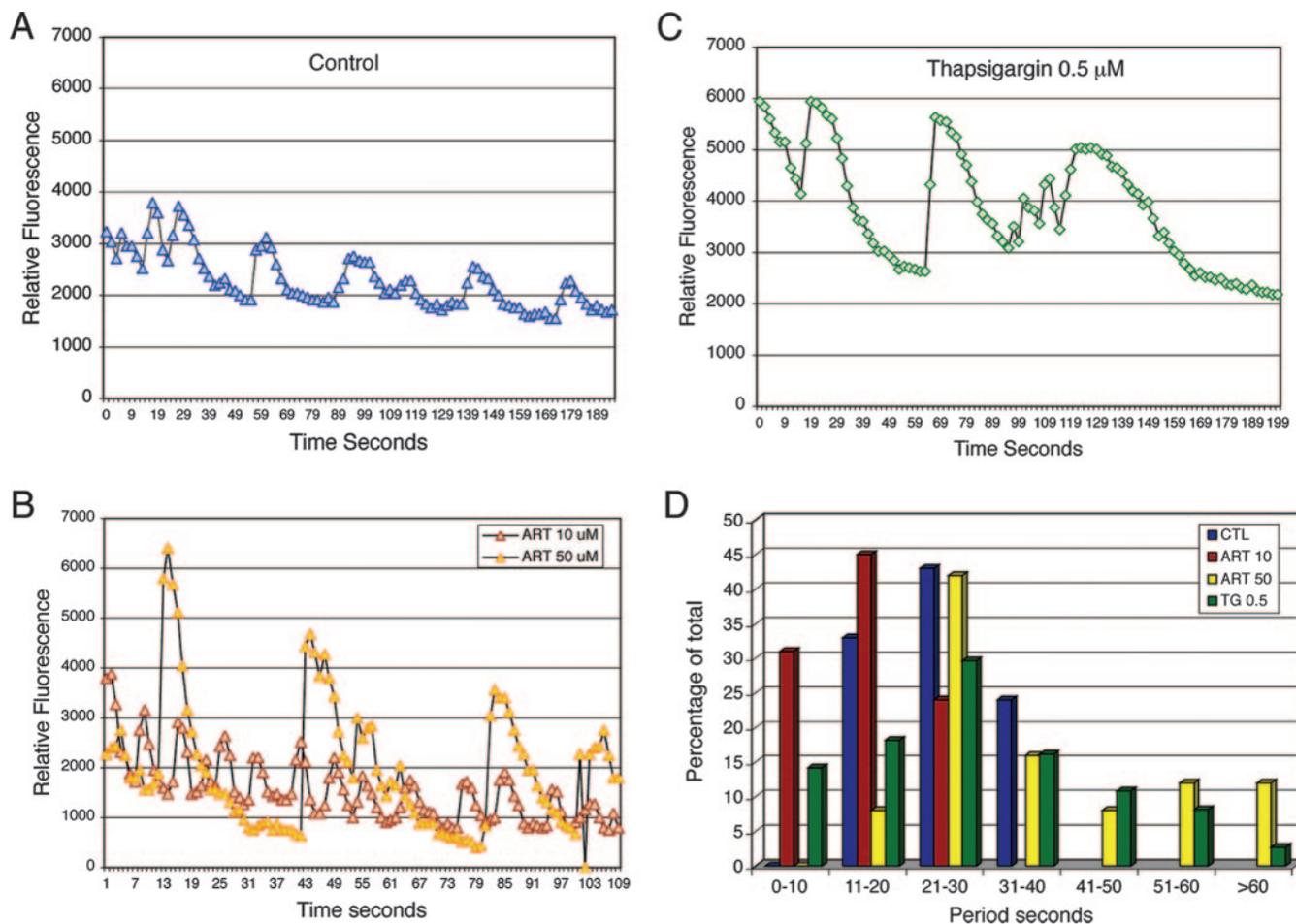
FIG. 6. Calcium oscillations in *T. gondii* induced by artemisinin or thapsigargin. Fluo-4-loaded parasites were imaged by using time-lapse fluorescence video microscopy, and the relative intensity of fluorescence, reflecting intracellular calcium levels, was plotted versus time. (A) Control cells showed repeated oscillations. (B) Treatment with 10 μM artemisinin (red) resulted in more rapid oscillations of similar amplitude but shorter period compared to the control. Treatment with 50 μM artemisinin (yellow) resulted in slower oscillations of much higher amplitude and longer period. (C) Treatment with 0.5 μM thapsigargin resulted in elevated average levels of calcium and in both slow calcium spikes of higher amplitude and short rapid oscillations. (D) Histogram analysis of the periodicity of cycles exhibited by control cells (blue, CTL), 10 μM artemisinin (red, ART 10), 50 μM artemisinin (yellow, ART 50), and 0.5 μM thapsigargin (green, TG 0.5).

doses of thapsigargin (0.5 μM) induced both more rapid, shallow oscillations and longer spikes with greater amplitude, leading to a broad distribution of cycles (Fig. 6D). Collectively, these results confirm that artemisinin and thapsigargin cause similar changes in calcium oscillations, inducing both rapid shallow oscillations and prolonged spikes in intracellular calcium.

DISCUSSION

We have explored the function of the Ca^{2+} ATPase SERCA in *T. gondii* in order to determine its role in calcium homeostasis and to investigate the molecular basis of inhibition by several plant sesquiterpene lactones. Our results indicate that *T. gondii* has a single functional SERCA based on the following evidence: (i) BLASTP similarity and phylogenetic grouping with known SERCA enzymes (36), (ii) conserved domain structure and presence of critical Ca^{2+} binding and ATPase residues, (iii) functional rescue of yeast cells defective in Ca^{2+} ATPases, and (iv) inhibition by thapsigargin, a known inhibitor

of SERCA Ca^{2+} ATPases (38). TgSERCA is localized to the ER of *T. gondii*, where it likely participates in controlling calcium stores that are important for microneme secretion and motility. We also demonstrate that artemisinin (i) triggers calcium-dependent secretion of microneme proteins in *T. gondii*, (ii) inhibits the functional rescue of yeast mutants expressing TgSERCA, and (iii) induces sustained calcium spikes in *T. gondii*. Collectively, our studies indicate that artemisinin affects calcium homeostasis and signaling in the parasite, supporting the conclusions that it acts as an inhibitor of SERCA.

T. gondii has a highly polarized secretory pathway with the ER being an extension of the nuclear envelope: the major site of exit from the ER occurs at the apical surface of the nuclear envelope, leading to a juxtanuclear, stacked Golgi and extending to apical secretory organelles (17). Immunolabeling of TgSERCA confirmed it is located in the ER, where it largely overlaps with GFP containing the C-terminal ER retention sequence HDEL. Surprisingly, the distribution of TgSERCA was somewhat different in extracellular parasites, where the protein was partially found in

apical membranes that were localized near micronemes. This pattern was not shared by GFP-HDEL, which was retained near the nuclear envelope, suggesting that the ER becomes partitioned in extracellular parasites. Other cells also develop specialized membranes in locations that are important for local calcium control. For example, SERCA orthologues are present in the vacuole in plant cells (37) and alveolar sacks in ciliates (22). The distribution of the TgSERCA-containing vesicles to the apex may be important for rapid release and effective recovery of cytosolic Ca^{2+}, events that likely govern both motility and microneme secretion.

Artemisinin treatment of *T. gondii* resulted in calcium-dependent secretion of microneme proteins as detected by release of MIC2 into the supernatant, similar to the SERCA inhibitor thapsigargin. While artemisinin treatment was less potent than thapsigargin, it exhibited a dose- and time-dependent induction of microneme secretion in *T. gondii*. Induction of microneme secretion by both artemisinin and thapsigargin was inhibited by chelation of intracellular calcium, while being much less influenced by extracellular calcium. These results are consistent with both agents acting to release intracellular calcium stores, thus leading to elevated cytosolic calcium that triggers microneme secretion. TgSERCA was shown to complement a yeast strain that is defective in Ca^{2+} transport, thus establishing it is a functional Ca^{2+} transporter. TgSERCA expressed in this heterologous system was sensitive to thapsigargin, similar to SERCA orthologues in animal cells. The ability of TgSERCA to complement deficient yeast was also inhibited by artemisinin. The potency of artemisinin in inhibiting the complementation of K616 yeast by TgSERCA and in stimulating parasite secretion was similar, suggesting it acts on the parasite by inhibiting SERCA.

Thapsigargin inhibits SERCA by locking it in the E2 conformation, thus preventing calcium pumping (38, 39). Inhibition of SERCA would be expected to prevent the reuptake into the ER, resulting in higher cytosolic calcium levels. Previous studies of pancreatic B cells have shown that calcium oscillations can be perturbed by thapsigargin, resulting in a pattern of stronger calcium spikes (16). A similar response to treatment with thapsigargin was apparent in Fluo-4 monitoring of calcium levels in *T. gondii* in the present study. While artemisinin did not lead to higher resting levels of $[Ca^{2+}]_i$, it did profoundly increase the periodicity and duration of calcium spikes in *T. gondii*. This behavior mimics the effects of thapsigargin on calcium oscillations by *T. gondii*, although thapsigargin was considerably more potent. The reason why the two compounds result in different profiles of calcium oscillations is uncertain but could result from differences in binding to the target and thus how they affect the cycling between the E1 and E2 conformations of the SERCA pump.

Previous studies have shown that during gliding motility, $[Ca^{2+}]_i$ levels in *T. gondii* undergo periodic oscillations that are dramatically dampened during cell invasion (27). Calcium oscillations are a common phenomenon during fertilization, cell migration, and during the cell cycle in a variety of vertebrate systems from frogs to humans (2). The molecular basis of the oscillations seen in *Toxoplasma* is not known, although they suggest a simple two-component circuit consisting of a calcium release channel and a reuptake pump (SERCA). The source for the increase in cytoplasmic calcium is from an intracellular pool, since the periodicity and amplitude of calcium oscillations were not affected by removal of calcium from the medium. Calcium release channels have not yet been characterized in *T. gondii*, or for that matter in yeast, protozoa, or plants, and these organisms do not contain conserved calcium release channels typical of animal cells (36, 37). The control of calcium homeostasis is likely to be complex since *T. gondii* also contains several other P-type Ca^{2+} ATPases (36), as well as other cation exchangers (http://ToxoDB.org).

Artemisinin and its derivatives have been used widely as a therapy for malaria, owing to their extremely potent inhibition of the parasite (18). This activity may be due to inhibition of the parasite SERCA as demonstrated by expression studies in *Xenopus* (12). In these heterologous systems, artemisinins are highly selective for malaria SERCA versus mammalian enzymes, presumably due to molecular differences in the binding site within the calcium channel of SERCA (47). Toxoplasma is also much less sensitive to artemisinin than malaria (19, 20), although newer variants such as artemisone are considerably more potent against both organisms (18, 35). Interestingly, another plant product, ryanodine, also disrupts calcium homeostasis in *T. gondii* (26); however, its target is calcium release channels in the ER rather than the reuptake pump SERCA. Because these agents disrupt calcium homeostasis at opposing points (i,e., release versus uptake), their collective action might be expected to be synergistic. Collectively, our findings indicate an important role for calcium regulation in the Apicomplexa and support the idea that calcium pumps and channels are important potential drug targets in parasites.

REFERENCES

1. **Berridge, M. J., M. D. Bootman, and H. L. Roderick.** 2003. Calcium signaling: dynamics, homeostasis and remodeling. Nat. Rev. Mol. Cell Biol. **4:**517–529.
2. **Berridge, M. J., P. Lipp, and M. D. Bootman.** 2000. The versatility and universality of calcium signaling. Nat. Rev. Mol. Cell. Biol. **1:**11–21.
3. **Carruthers, V. B.** 2002. Host cell invasion by the opportunistic pathogen *Toxoplasma gondii*. Acta Trop. **81:**111–122.
4. **Carruthers, V. B., S. N. J. Moreno, and L. D. Sibley.** 1999. Ethanol and acetaldehyde elevate intracellular $[Ca^{2+}]$ calcium and stimulate microneme discharge in *Toxoplasma gondii*. Biochem. J. **342:**379–386.
5. **Carruthers, V. B., G. D. Sherman, and L. D. Sibley.** 2000. The Toxoplasma adhesive protein MIC2 is proteolytically processed at multiple sites by two parasite-derived proteases. J. Biol. Chem. **275:**14346–14353.
6. **Carruthers, V. B., and L. D. Sibley.** 1999. Mobilization of intracellular calcium stimulates microneme discharge in *Toxoplasma gondii*. Mol. Microbiol. **31:**421–428.
7. **Chen, X. M., S. P. O'Hara, B. Q. Huang, J. B. Nelson, J. J. C. Lin, G. Zhu, H. D. Ward, and N. F. LaRusso.** 2004. Apical organelle discharge by *Cryptosporidium parvum* is temperature, cytoskeleton, and intracellular calcium dependent and required for host cell invasion. Infect. Immun. **72:**6806–6816.
8. **Chini, E. N., K. Nagamune, D. M. Wetzel, and L. D. Sibley.** 2005. Evidence that the cADPR signaling pathway controls calcium-mediated secretion in *Toxoplasma gondii*. Biochem. J. **389:**269–277.
9. **Cunningham, K. W., and G. R. Fink.** 1994. Calcineurin-dependent growth control in *Saccharomyces cerevisiae* mutants lacking PMC1, a homolog of plasma membrane Ca^{2+} ATPases. J. Cell Biol. **124:**351–363.
10. **Dobrowolski, J. M., and L. D. Sibley.** 1996. *Toxoplasma* invasion of mam-

malian cells is powered by the actin cytoskeleton of the parasite. Cell **84:**933–939.

11. Dyer, M., M. Jackson, C. McWhinney, G. Zhao, and R. Mikkelsen. 1996. Analysis of a cation-transporting ATPase of *Plasmodium falciparum.* Mol. Biochem. Parasitol. **78:**1–12.

12. Eckstein-Ludwig, U., R. J. Webb, I. D. A. van Goethem, J. M. East, A. G. Lee, M. Kimura, P. M. O'Neill, P. G. Bray, S. A. Ward, and S. Krishna. 2003. Artemisinins target the SERCA of *Plasmodium falciparum.* Nature **424:**957–961.

13. Furuya, T., M. Okura, F. A. Ruiz, D. A. Scott, and R. Docampo. 2001. *TcSCA* complements yeast mutants defective in Ca^{2+} encodes a Ca^{2+}-ATPase that localizes to the endoplasmic reticulum of *Trypanosoma cruzi.* J. Biol. Chem. **276:**32437–32445.

14. Gantt, S., C. Persson, K. Rose, A. J. Birkett, B. Abagyan, and V. Nussenzweig. 2000. Antibodies against thrombospondin-related anonymous protein do not inhibit *Plasmodium* sporozoite infectivity in vivo. Infect. Immun. **68:**3667–3673.

15. Gee, K. R., K. A. Brown, W. N. Chen, J. Bishop-Stewart, D. Gray, and I. Johnson. 2000. Chemical and physiological characterization of Fluo-4 Ca^{2+}-indicator dyes. Cell Calcium **27:**97–106.

16. Gilon, P., A. Arredouani, P. Gailly, J. Gromada, and J. C. Henquin. 1999. Uptake and release of Ca^{2+} by the endoplasmic reticulum contribute to the oscillations of the cytoplasmic Ca^{2+} concentration triggered by Ca^{2+} influx in the electrically excitable pancreatic B-cell. J. Biol. Chem. **274:**20197–20205.

17. Hager, K. M., B. Striepen, L. G. Tilney, and D. S. Roos. 1999. The nuclear envelope serves as an intermediary between the ER and Golgi complex in the intracellular parasite *Toxoplasma gondii.* J. Cell Sci. **112:**2631–2638.

18. Haynes, R. K., and S. Krishna. 2004. Artemisinins: activities and actions. Microb. Infect. **6:**1339–1346.

19. Holfels, E., J. McAuley, D. Mack, W. K. Milhous, and R. McLeod. 1994. In vitro effects of artemisinin ether, cycloguanil hydrochloride (alone and in combination with sulfadiazine), quinine sulfate, mefloquine, primaquine phosphate, trifluoperazine hydrochloride, and verapamil on *Toxoplasma gondii.* Antimicrob. Agents Chem. **38:**1392–1396.

20. Jones-Brando, L., J. D'Angelo, G. H. Posner, and R. H. Yolken. 2006. In vitro inhibition of *Toxoplasma gondii* by four new derivatives of artemisinin. Antimicrob. Agents Chem. **50:**4206–4208.

21. Kimura, M., Y. Yamaguchi, S. Takada, and K. Tanabe. 1993. Cloning of a Ca^{2+}-ATPase gene of *Plasmodium falciparum* and comparison with vertebrate Ca^{2+}-ATPases. J. Cell Sci. **104:**1129–1136.

22. Kissmehl, R., S. Huber, B. Kottwitz, K. Hauser, and H. Plattner. 1998. Subplasmalemmal Ca-stores in *Paramecium tetraurelia.* Identification and characterisation of a sarco(endo)plasmic reticulum-like Ca^{2+}-ATPase by phosphoenzyme intermediate formation and its inhibition by caffeine. Cell Calcium. **24:**193–203.

23. Kuranda, K., V. Leberre, S. Sokol, G. Palamarczyk, and J. Francois. 2006. Investigating the caffeine effects in the yeast *Saccharomyces cerevisiae* brings new insights into the connection between TOR, PKC and Ras/cAMP signaling pathways. Mol. Microbiol. **61:**1147–1166.

24. Li, W., W. Mo, D. F. Shen, L. Sun, J. Wang, J. Lu, J. M. Gitchier, and B. Zhou. 2005. Yeast model uncovers dual roles of mitochondria in action of artemisinin. PLoS Genetics **1:**e36.

25. Liang, F., K. W. Cunningham, J. F. Harper, and H. Sze. 1997. ECA1 complements yeast mutants defective in Ca^{2+} pumps and encodes an endoplasmic reticulum-type Ca^{2+}-ATPase in *Arabidopsis thaliana.* Proc. Natl. Acad. Sci. USA **94:**8579–8584.

26. Lovett, J. L., N. Marchesini, S. N. Moreno, and L. D. Sibley. 2002. *Toxoplasma gondii* microneme secretion involves intracellular Ca^{2+} release from IP_3/ryanodine sensitive stores. J. Biol. Chem. **277:**25870–25876.

27. Lovett, J. L., and L. D. Sibley. 2003. Intracellular calcium stores in *Toxoplasma gondii* govern invasion of host cells. J. Cell Sci. **116:**3009–3016.

28. Luo, S., F. A. Ruiz, and S. N. Moreno. 2005. The acidocalcisome Ca^{2+} ATPase (TgA1) of *Toxoplasma gondii* is required for polyphosphate storage,

intracellular calcium homeostasis and virulence. Mol. Microbiol. **55:**1034–1045.

29. Luo, S., M. Vieira, J. Graves, L. Zhong, and S. N. Moreno. 2001. A plasma membrane-type Ca^{2+}-ATPase colocalizes with a vacuolar H^+-pyrophosphatase to acidocalcisomes of *Toxoplasma gondii.* EMBO J. **20:**55–64.

30. Melo, E. J. L., M. Attias, and W. De Souza. 2000. The single mitochondrion of tachyzoites of *Toxoplasma gondii.* J. Struct. Biol. **130:**27–33.

31. Mishina, Y. V., S. Krishna, R. K. Haynes, and J. C. Meade. 2007. Artemisinins inhibit *Trypanosoma cruzi* and *Trypanosoma rhodesiense* in vitro growth. Antimicrob. Agents Chemo. **51:**1852–1854.

32. Moreno, S. N. J., and R. Docampo. 2003. Calcium regulation in protozoan parasites. Curr. Opin. Microbiol. **6:**359–364.

33. Moreno, S. N. J., and L. Zhong. 1996. Acidocalcisomes in *Toxoplasma gondii* tachyzoites. Biochem. J. **313:**655–659.

34. Moudy, R., T. J. Manning, and C. J. Beckers. 2001. The loss of cytoplasmic potassium upon host cell breakdown triggers egress of *Toxoplasma gondii.* J. Biol. Chem. **276:**41492–41501.

35. Nagamune, K., S. N. J. Moreno, and L. D. Sibley. 2007. Artemisinin-resistant mutants of *Toxoplasma gondii* have altered calcium homeostasis. Antimicrob. Agents Chemother. **51:**3816–3823.

36. Nagamune, K., and L. D. Sibley. 2006. Comparative genomic and phylogenetic analyses of calcium ATPases and calcium-regulated proteins in the Apicomplexa. Mol. Biol. Evol. **23:**1613–1627.

37. Nagata, T., S. Iizumi, K. Satoh, H. Ooka, J. Kawai, P. Carninci, Y. Hayashizaki, Y. Otomo, K. Murakami, K. Matsubara, and S. Kikuchi. 2004. Comparative analysis of plant and animal calcium signal transduction element using plant full-length cDNA data. Mol. Biol. Evol. **21:**1855–1870.

38. Sagara, Y., and G. Inesi. 1991. Inhibition of the sarcoplasmic reticulum Ca^{2+} transport ATPase by thapsigargin at subnanomolar concentrations. J. Biol. Chem. **266:**13503–13506.

39. Sagara, Y., J. B. Wade, and G. Inesi. 1992. A conformational mechanism for formation of a dead-end complex by the sarcoplasmic reticulum ATPase with thapsigargin. J. Biol. Chem. **267:**1286–1292.

40. Sarciron, M. E., C. Saccharin, A. F. Petavy, and F. Peyron. 2000. Effects of artesunate, dihydroartemisinin, and an artesunate-dihydroartemisinin combination against *Toxoplasma gondii.* Am. J. Trop. Med. Hyg. **62:**73–76.

41. Sibley, L. D. 2004. Invasion strategies of intracellular parasites. Science **304:**248–253.

42. Sorensen, T. L. M., J. V. Moller, and P. Nissen. 2004. Phosphoryl transfer and calcium ion occlusion in the calcium pump. Science **304:**1672–1675.

43. Thastrup, O., P. J. Cullen, B. K. Drobak, M. R. Hanley, and A. P. Dawson. 1990. Thapsigargin, a tumor promotor, discharges intracellular Ca^{2+} stores by specific inhibition of the endoplasmic reticulum Ca^{2+}-ATPase. Proc. Natl. Acad. Sci. USA **87:**2766–2770.

44. Toyoshima, C., and G. Inesi. 2004. Structural basis of ion pumping by Ca^{2+}-ATPase of the sarcoplasmic reticulum. Annu. Rev. Biochem. **73:**269–292.

45. Toyoshima, C., and T. Mizutani. 2004. Crystal structure of the calcium pump with a bound ATP analogue. Nature **430:**529–535.

46. Toyoshima, C., M. Nakasako, H. Nomura, and H. Ogawa. 2000. Crystal structure of the calcium pump of sarcoplasmic reticulum at 2.6 Å resolution. Nature **405:**647–655.

47. Uhlemann, A. C., A. Cameron, U. Eckstein-Ludwig, J. Fischbarg, P. Iserovich, F. A. Zuniga, M. East, A. Lee, L. Brady, R. K. Haynes, and S. Krishna. 2005. A single amino acid residue can determine the sensitivity of SERCAs to artemisinins. Nat. Struct. Mol. Biol. **12:**628–629.

48. Vieira, M. C. F., and S. N. J. Moreno. 2000. Mobilization of intracellular calcium upon attachment of *Toxoplasma gondii* tachyzoites to human fibroblasts is required for invasion. Mol. Biochem. Parasit. **106:**157–162.

49. Wetzel, D. M., L. A. Chen, F. A. Ruiz, S. N. J. Moreno, and L. D. Sibley. 2004. Calcium-mediated protein secretion potentiates motility by *Toxoplasma gondii.* J. Cell Sci. **117:**5739–5748.

50. Wuytack, F., L. Raeymaekers, and L. Missiaen. 2002. Molecular physiology of the SERCA and SPCA pumps. Cell Calcium **35:**279–305.